

# Journal of Materials Chemistry B

Accepted Manuscript



This is an *Accepted Manuscript*, which has been through the Royal Society of Chemistry peer review process and has been accepted for publication.

*Accepted Manuscripts* are published online shortly after acceptance, before technical editing, formatting and proof reading. Using this free service, authors can make their results available to the community, in citable form, before we publish the edited article. We will replace this *Accepted Manuscript* with the edited and formatted *Advance Article* as soon as it is available.

You can find more information about *Accepted Manuscripts* in the [Information for Authors](#).

Please note that technical editing may introduce minor changes to the text and/or graphics, which may alter content. The journal's standard [Terms & Conditions](#) and the [Ethical guidelines](#) still apply. In no event shall the Royal Society of Chemistry be held responsible for any errors or omissions in this *Accepted Manuscript* or any consequences arising from the use of any information it contains.



## Hydroxyapatite Nanowhiskers Embedded in Chondroitin Sulfate Microspheres as Colon Targeted Drug Delivery System

Received 00th January 20xx,  
Accepted 00th January 20xx

DOI: 10.1039/x0xx00000x

www.rsc.org/

T. S. P. Cellet, G. M. Pereira, E. C. Muniz, R. Silva\* and A. F. Rubira

An inorganic/organic hybrid material with triggering mechanism for specific drug delivery at colon is demonstrated. First, hydroxyapatite nanowhiskers (n-HA) with high aspect ratio, narrow particle size distribution and high surface area, ca. 67 m<sup>2</sup>/g, are prepared. As a *proof-of-concept*, terbinafine, a fungicidal agent, is loaded onto the n-HA, obtaining a drug loading of 40.63 mg of terbinafine per gram of n-HA. Hydroxyapatite nanowhiskers loaded with terbinafine are encapsulated with chondroitin sulfate (CS) microspheres, using chemically modified glycidyl methacrylate by performing ultrasonic microemulsion polymerization. The obtained hybrid materials were characterized by TEM, SEM, FTIR, and NMR. Dispersed n-HA in CS microspheres are obtained for different n-HA contents, from 1 to 10% (%w/w). Terbinafine release from hybrid microspheres is carried out by *in vitro* studies in simulated gastric fluid and simulated intestinal fluid. The studies demonstrated that sustained drug release can be obtained using the developed hybrid material.

### 1. Introduction

Drug delivery systems (DDS) with specific release triggering mechanism that can also provide sustained drug delivery pattern at specific body environment can improve the efficiency of drugs and reduce their side effects.<sup>1,2</sup> Along with specific targeting mechanism, the associated toxicity of the degraded products of the carrier system is a serious concern.<sup>3,4</sup> Multifunctional materials with features that can endorse its application as DDS can arise from the combination of inorganic and organic materials.<sup>5</sup>

High surface area inorganic materials, frequently used as adsorbents, when associated with stimuli-responsive polymeric materials end up to be fascinating vehicles for specific drug delivery system.<sup>6,7</sup> However, having inorganic and organic phases associated in a synergistic way depends on the interaction among the phases, as well as the system dimensions and morphology. For this purpose, the synthesis of designed hybrid materials that take advantage of both phases demands feasible production methodologies.

Calcium phosphates (CaP) are appealing inorganic candidates for DDS, due their low or none toxicological response, even upon degradation. CaP degrades into Ca<sup>2+</sup> and PO<sub>4</sub><sup>3-</sup> ions. These same ions are already present in elevated concentration in living organisms.<sup>8,9</sup> However, the direct use of CaP nanoparticles are not suitable due particles aggregation and

growth during drug incorporation or during storage.<sup>10,11</sup> CaP are found in many different phases in function of crystal structure or stoichiometry.<sup>12</sup> CaP have high biotechnological importance since they are the main constitutive compounds of bones tissues, where several CaP phases can co-exist.<sup>13</sup> Among all CaP phases, hydroxyapatite (HA) is one of the most significant phase due its stability and extended biocompatibility.<sup>14</sup> HA has lower solubility and higher stability in comparison to other CaP, i.e. the solubility product of HA is more than thirty orders of magnitude lower than  $\alpha$ -Tricalcium phosphate ( $\alpha$ -TCP).<sup>15</sup> Another HA important feature is its capability to form different particles shapes and sizes according to the synthetic method used.

HA nanoparticles have important features that make them useful as adsorbent, such as their high surface to volume ratio, surface reactivity and biomimetic morphologies. Therefore, n-HA is frequently used in applications as adsorbent during chromatography for purification and separation, and also in applications as implant coating or bone substitute filler.<sup>16,17</sup>

Development of DDS technology is one of the main research areas in science in which polymeric materials have played a major role. The vast variation of polymers properties, according to composition or structural features, is a pool full of opportunity to develop new materials to use in human health care issues.<sup>18</sup> Polymer can be used in a DDS to provide a triggering mechanism to promote drug delivery at specific environment. For instance, chondroitin sulfate (CS), a natural polymer, degrades in the colon by the action of specific bacteria. Since CS is not digested in the stomach or in the small intestine, it can be used as organic phase in a DDS to allow drug delivery in the colon by oral admission.<sup>19,20</sup> Glycosaminoglycans polymers, such as CS, are present in

Departamento de Química, Universidade Estadual de Maringá, Avenida Colombo 5790, CEP: 87020-900 - Maringá, Paraná, Brazil.  
Electronic Supplementary Information (ESI) available. See  
DOI: 10.1039/x0xx00000x

connective tissues of animals and these natural polymers can be produced at large scale using simple processes. CS has shown high biocompatibility in diverse studies and it does not offer problems of bioaccumulation and biodegradability.<sup>21</sup> The use of soluble polymers, i.e CS, in formulation of oral DDS is possible by the modification of the polymer backbone. Moieties able to promote polymer cross-linking or with features to establish strong intramolecular interaction can be inserted to the polymers backbone to avoid the dissolution of polymers microspheres.<sup>22,23</sup>

In the present study, we demonstrated the synthesis of hydroxyapatite by a wet method that lead to the formation of particles with peculiar aspect ratio and whisker-like particles shape. Adsorption of terbinafine, a fungicidal agent, is carried out using n-HA as adsorbent. Inorganic material loaded with the drug is applied to the synthesis of CS microspheres with different content of inorganic phase from 1 to 10% (in weight). The synthesis of CS microspheres is performed by the chemical modification of CS backbone with glycidyl methacrylate (GMA) aiming the introduction of vinyl pendent groups. Then, during microspheres synthesis, these vinyl groups are used to promote intra and intermolecular cross-linking of CS chains, forming stable microspheres in aqueous media. Polymer microspheres are desired system for controlled release formulations because they offer various advantages in view of their well defined release pattern and stability in different media<sup>24</sup>. Usually, the interaction of the particles with biologic system depends also on the particle size.<sup>25</sup> Therefore, preparation methods that lead to mono disperse microsphere are needed to produce microspheres suitable for drug delivery applications.<sup>26</sup> Among the methods available to produce polymer microspheres, cross-link polymerization in micro emulsion is used herein. In this method, the microsphere preparation and filler incorporation takes place in a single process. It can be used for loading of filler controlling the filler content and it provides better dispersion of the filler in the polymeric matrix.<sup>27</sup>

Our aim in the present study is the development of a DDS as a terbinafine delivery carrier that not only has efficient drug adsorption/release ability but also shows excellent biocompatibility. For this purpose, nanosized HA coated with CS microspheres were prepared with a series of n-HA contents (1%, 3%, 5%, 7% and 10 %) using water/benzyl alcohol emulsion method. Terbinafine release from hybrid microspheres is carried out by *in vitro* studies in simulated gastric fluid (SGF) and simulated intestinal fluid (SIF).

## 2. Experimental

### 2.1. Materials

Chondroitin sulfate (CAS 9007-28-7) with Mw of 20,000 g/mol determined by GPC/SEC was kindly supplied by Solabia, Brazil. CS utilized in this work is a mixture of CS sulfated in the C4 and C6 positions. Cellulose membranes for dialysis with molecular weight cut-off (MWCO) at 12,000 (Sigma–Aldrich Co., New Delhi, India) were used for *in vitro* release tests. Ethanol 99.5%

(Nuclear-Brazil, CAS 64-17-5), acetone (Fmaia-Brazil, CAS 67-64-1), ammonium hydroxide (Nuclear-Brazil, CAS 1336-21-6), benzyl alcohol 99.8% (Fmaia-Brazil, CAS 100-51-6), calcium hydroxide (Sigma-Aldrich, CAS 1305-62-0), glycidyl methacrylate 97% (Aldrich, CAS 106-91), hydrochloric acid 37% (Fmaia-Brazil, 7647-01-0), phosphoric acid 85% (Fmaia-Brazil, CAS 7664-38-2), sodium persulfate ≥ 98%, (Aldrich, CAS 7775-27-1), terbinafine hydrochloride ≥98% (Sigma-Aldrich, CAS 78628-80-5) were used as received.

### 2.2. Method

**2.2.1. Synthesis of Hydroxyapatite Nanowhiskers (n-HA).** n-HA with Ca/P ratio of 1.67 were synthesized by a wet chemical precipitation reaction between Ca(OH)<sub>2</sub> and H<sub>3</sub>PO<sub>4</sub>. Ca(OH)<sub>2</sub> powder was slowly added into 100 mL of deionized water at 25 °C. The mixture was vigorously agitated for one hour to prepare a 0.5 mol/L Ca(OH)<sub>2</sub> suspension. Then 100 mL of H<sub>3</sub>PO<sub>4</sub> 0.3 mol/L was added dropwise into Ca(OH)<sub>2</sub> suspension with a ratio of approximately 6 mL/min to produce a white precipitate. The mixture pH was kept at 8.0±1.0 during the addition of acid to the Ca(OH)<sub>2</sub> suspension by the addition of 1.0 mol/L NH<sub>4</sub>OH solution. The mixture was kept at room temperature for 24 h. The precipitate was separated from the supernatant by filtration, washed for three consecutive times with deionized water and dried at 75 °C for 12 h. The obtained powdered material was calcined at 900 °C for 8 h. After calcination, the solid were milled and passed through a 200 mesh sieve.

**2.2.2 Adsorption of Terbinafine on Hydroxyapatite nanowiskers (HA-TB).** Adsorption experiments were performed according to the reported by Kojima et al.<sup>28</sup> In brief, it was prepared a solution of TB containing 2.5 mg/mL in ethanol/water mixtures (5.5/4.5 v/v). An appropriated amount of n-HA was added to TB solution to result in a 5% of TB/n-HA weight ratio. The suspensions were stirred for 5 h and centrifuged. Therefore, the amount of terbinafine adsorbed on the n-HA particles can be calculated as the difference of the initial amount of terbinafine in the solution to the residual amount after the adsorption experiment. The encapsulation efficiency (EE) of the terbinafine is defined as the percentage of drug incorporated onto the nanowhiskers in relation to the total drug added. The amount of drug loaded into n-HA was determined by the analysis of the supernatant obtained after the adsorption of terbinafine in the n-HA. The supernatant contains the drug not encapsulated in nanowhiskers and the concentration of terbinafine can determined using UV-Vis spectrophotometer ((Model 800Xi, Femto-Brazil) at 222 nm. The EE was determined using the following equation:<sup>29-31</sup>

$$\text{Encapsulation efficiency (EE \%)} = \frac{(\text{Total TB (mg)}) - (\text{Residual TB present in supernatant(mg)})}{\text{Total TB (mg)}} \times 100$$

**2.2.3. Synthesis of chondroitin sulfate-methacrylate (CS-methacrylate).** The methodology to prepare CS-methacrylate was adapted from the literature.<sup>32, 33</sup> 8.32 g of CS was dissolved in 150 mL of water at room temperature for 2 h. The solution pH was adjusted to 3.5 by the addition of HCl 0.1 mol/L. Then, 2.7 mL of GMA was poured to the reaction

system. The reaction system was heated to 50 °C and kept under magnetic stirring for 24 h. At room temperature, CS-methacrylate was precipitated by the addition of 300 mL of ethanol. CS-methacrylate was recovered by centrifugation at 9000 rpm and 20 °C. CS-methacrylate was copiously washed with ethanol to remove unreacted substances. CS-methacrylate was purified by dialysis using deionized water at 5 °C for 72 h. After, the material was lyophilized at -55 °C for 24 h to yield a white powder.

**2.2.4. Synthesis of CS-methacrylate microspheres cross-linked by ultrasound with hydroxyapatite nanowhiskers loaded with terbinafine (CS-methacrylate-HA-TB).** 23 mg of sodium persulfate ( $\text{Na}_2\text{S}_2\text{O}_8$ ) was added to 15 mL of aqueous solution of CS-methacrylate 15 % (w/v). HA-TB nanowhiskers were dispersed in the previous solution with at different mass ratio (0, 1, 3, 5, 7 and 10%) in relation to the total amount of CS-methacrylate. The obtained aqueous dispersion were poured into 45 mL of benzyl alcohol (water to benzyl alcohol ratio of 1:3) resulting in a two-phase system with alcoholic portion being the continuous phase. The water/benzyl alcohol mixture was sonicated with the use of an ultrasonic oscillation probe (Cole-Parmer® 500, model EW-04711-40), applying a frequency of 20 kHz for 60 s. 20  $\mu\text{L}$  of  $\text{N,N',N'}$ -Tetramethylethylenediamine (TEMED) was added as catalyst. The product was precipitated in acetone and separated by centrifugation at 10000 rpm for 20 minutes. After the emulsion polymerization the material was precipitated in acetone. Acetone was used due the higher miscibility of benzyl alcohol and acetone, and due to the fact that the polymer matrix is not soluble in acetone. The solid materials were recovered by centrifugation at 10.000 rpm for 10 min and washed three times with acetone to complete benzyl alcohol removal. After washed and centrifugation, the solid was dried at room temperature and then lyophilized at -55 °C for 24h. The complete removal of benzyl alcohol and acetone from the samples were proved by solid state NMR ( $^{13}\text{C}/\text{CP-MAS}$ ), where the characteristics peaks of the solvent are completely absent.

**2.2.5. Dispersion of n-HA and n-HA-CS microspheres.** 10 mg n-HA nanowhiskers or n-HA-CS microspheres containing 1%, 3%, 5%, 7% and 10 % (w/w) of n-HA nanowhiskers was added to 3 mL of deionized water. The suspensions were sonicated for 30 min and then digital images were taken after 1 minute and 1 hour of resting time.

**2.2.6. Terbinafine release from n-HA-CS microspheres in simulated gastric fluid (SGF) and simulated intestinal fluid (SIF).** The *in vitro* release tests were performed in a tablets and capsules dissolution tester (Model 299, Ethik Technology Equipment Solutions). The release assays were carried under mechanical stirring of 60 rpm and constant temperature of 36.5 °C. At predetermined intervals times, aliquots of the solution were collected to determine the concentration of terbinafine released. The terbinafine concentration was determined by UV-VIS spectrophotometer (Model 800Xi, Femto-Brazil) using the solution absorbance at 222 nm. Terbinafine (TB) release assays were performed in both simulated gastric fluid (SGF, 2.0 g NaCl and 7.0 mL of concentrated aqueous solution of HCl 37% (v/v) in 1000 mL of

water, pH = 1.2) and simulated intestinal fluid (SIF, 6.8 g of  $\text{KH}_2\text{PO}_4$  and 77 mL of aqueous NaOH 0.20 mol.L<sup>-1</sup> in 1000 mL of water, pH = 6.8).

In a release assay, 100 mg of sample was placed in a cellulose membrane containing 20 mL of SGF or SIF solutions. The membrane was tied and immersed in 130 mL of SGF or SIF solutions present in the dissolution tester. Aliquots of the solution used in the determination of TB concentration by UV-Vis were returned to the dissolutor. Concentration of TB released from microspheres was determined from an analytical curve correlating the absorbance versus the concentration of the drug in SGF solution. The regression coefficient ( $R^2$ ) of 0.9989 was obtained for the absorbance versus the concentration curve.

### 2.3. Characterizations

**2.3.1 Wide-angle X-ray diffraction (WAXD).** X-ray diffractograms of the samples were obtained from Shimadzu, Model D6000 equipped with a Cu-K $\alpha$  radiation source (30kV and 20 mA) and nickel filter operating in continuous mode. The diffractograms were recorded in the range from 5 to 60° with resolution of 0.02° and with scanning speed of 0.5 ° min<sup>-1</sup>. The crystallite size ( $L_c$ ) of hydroxyapatite after milling was estimated from the Scherrer's equation<sup>34,35</sup>:

$$L_c = \frac{k\lambda}{\beta_{hkl} \cos \theta}$$

where  $L_c$  is the average crystallite size (nm),  $\beta_{hkl}$  is the full width of the peak at half of the maximum intensity,  $\lambda$  is the wavelength of X-ray radiation and  $k$  is the shape coefficient (value between 0.9 and 1). The instrumental broadening  $\beta_{hkl}$  corresponding to the diffraction peak was estimated using the following equation<sup>36</sup>:

$$\beta_{hkl} = \sqrt{\beta_{exp}^2 - \beta_{inst}^2}$$

where  $\beta_{exp}$  corresponds to the experimental half width and  $\beta_{inst}$  the instrumental half width related to the powder standard LaB<sub>6</sub> (SRM 660-NIST). The crystallite size is a measurement of the size of coherently diffraction domains and it is not the same as particle size.

**2.3.2 FTIR spectroscopy.** Samples were characterized by infrared spectroscopy technique using a transform infrared spectrophotometer (Bomem FT-IR model MB100 spectrometer), operating in the region from 4000 to 400 cm<sup>-1</sup>, resolution of 4 cm<sup>-1</sup> with a total of 128 scans. Dried materials were blended with KBr powder and pressed into tablets before spectra acquisition.

**2.3.3  $^1\text{H-NMR}$  and solid-state  $^{13}\text{C-CP/MAS}$  NMR spectroscopies.**  $^1\text{H}$  NMR spectra were recorded on a Varian spectrometer, model Mercury Plus BB 300 MHz, by applying frequencies of 300.059 MHz. NMR spectra were obtained using approximately 10 mg of each sample dissolved in 0.7 mL of D<sub>2</sub>O containing 3-(trimethylsilyl)propionic-2,2,3,3-d<sub>4</sub> acid sodium salt ((TSP-d<sub>4</sub> (0.05%)) as internal reference. The parameters were set to angle pulse of 90 ° and relaxation time of 30 s.

Solid-state  $^{13}\text{C-CP/MAS}$  NMR spectra were obtained on a Varian Oxford 300 using frequency of 74.47 MHz, angle pulse

of 37°, frequency of 12 kHz, contact time of 3 ms, and relaxation time of 3 s.

**2.3.4 Scanning electron microscopy (SEM) and energy dispersive spectroscopy (EDS).** The morphologies of the samples were analyzed in a scanning electron microscope (Shimadzu, model SS 550 Superscan). The used parameters were acceleration voltage of 15 kV and current of 30 mA. The surfaces of the samples were previously coated with a thin layer of gold deposited by sputtering technique (model HF-50 ION COATER, Shimadzu).

**2.3.5 Transmission electron microscopy (TEM).** The micrographs of n-HA particles were obtained by transmission electron microscopy (JEM 1400, JEOL) applying an acceleration voltage of 120 kV. A suspension containing the samples was deposited on TEM grids (Carbon-Formvar-coated copper-400 mesh) and left to dry at room temperature.

**2.3.6 Measurements of N<sub>2</sub> adsorption and desorption.** For the analysis of N<sub>2</sub> adsorption, a pretreatment step was performed submitting the sample to 300 °C for 4 h under vacuum of 10 μmHg with heating rate of 1 °C/minute. Afterwards, is carried

out the sorption step using of N<sub>2</sub> gas with 99.999% purity at a temperature of 77 K. Data were obtained by Micromeritics equipment model ASAP2020. The surface area was calculated by Brunauer–Emmett–Teller (BET) method with a range of P/P<sub>0</sub> between 0.05 and 0.30. Pore size was calculated by using Barrett-Joyner-Halenda (BJH) method from the desorption branch.<sup>37,38</sup>

### 3. Results and discussion

#### 3.1. Synthesis of hydroxyapatite nanowhiskers (n-HA)

n-HA synthesis was carried out by a wet chemistry method using calcium hydroxide and phosphoric acid. Calcium hydroxide reacts with phosphoric acid producing a white precipitate, hydroxyapatite, according to reaction (1), wherein the ratio of calcium relative to phosphor (Ca/P) is adjusted to 1.67.

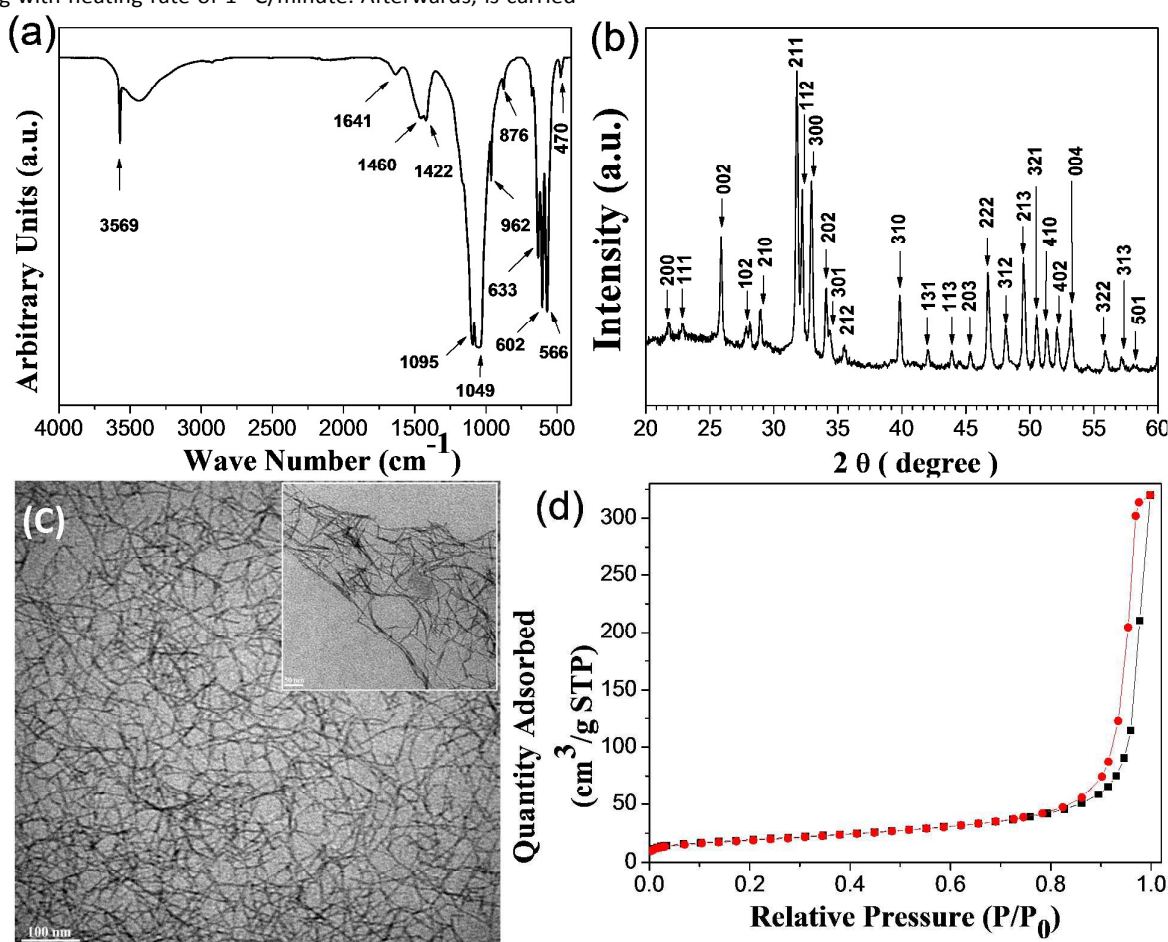
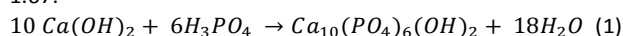


**Figure 1.** FTIR spectrum (a), X-ray diffraction patterns (b), Transmission electron microscopy (TEM) images (c) and N<sub>2</sub> adsorption/desorption isotherms of hydroxyapatite (n-HA) (d).

Hydroxyapatite synthesis was confirmed by FTIR, WAXD, BET and BJH, Figure 1. FTIR spectrum of as synthesized n-HA is shown in Figure 1a. Characteristic stretching mode of hydroxyl

groups in hydroxyapatite phase is observed at 3569 cm<sup>-1</sup>. Hydroxyl groups in hydroxyapatite phase can be easily differed from OH signal of adsorbed water, since it appears as a narrow peak in function of the well stabilized interactions of hydroxyls

ions in the hydroxyapatite lattice. In addition, phosphate ions have four active vibrational modes in IR ( $\nu_1$ ,  $\nu_2$ ,  $\nu_3$  and  $\nu_4$ ). All these modes are observed for n-HA in the FTIR spectrum.<sup>39,40</sup> In the FTIR spectrum of n-HA it is also observed the presence of carbonate ions. Carbonate ions have four vibration modes, three of them are observed in the FTIR spectrum. The carbonate  $\nu_4$  mode has very low intensity and it is seldom verified in the infrared spectrum.<sup>41</sup> FTIR spectrum of n-HA has peaks attributed to carbonate ions in the region of 1650 and 1300  $\text{cm}^{-1}$ . Three signals for  $\nu_3$  vibration mode are centered at 1641, 1460 and 1422  $\text{cm}^{-1}$ . These carbonate bands in the region of 1650 to 1300  $\text{cm}^{-1}$  are assigned to surface carbonate ions, rather than to carbonate ions in the lattice of phosphate ions. The presence of carbonate ions, mainly located at the surface of the hydroxyapatite particles, as pointed out by the FTIR result, can be justified by the dissolution of atmospheric  $\text{CO}_2$  in the acidified solution of phosphoric acid during the hydroxyapatite precipitation. Interestingly, hydroxyapatites from biologic sources also have carbonate ions as impurities. The obtaining of hydroxyapatite phase can also be confirmed by WAXD. In the Figure 1b, the XRD diffraction pattern of n-HA are presented. The peaks assignments were performed using the JCPDS card 09-0432. The diffractogram presents all peaks attributed to hydroxyapatite phase, such as (002), (211) and (300) at 25.6°, 31.8°, and 32.9°, respectively. The absence of amorphous halo or additional peaks not related to hydroxyapatite suggests that the synthesized materials consist of highly crystalline material without the presence of other phosphate phases.<sup>42-44</sup>

XRD peak broadening can be used to estimate the crystallite sizes along the perpendicular direction to the crystallographic plane, using the Scherrer's equation. The peaks referents to the (211) and (002) crystal plane were used for this estimation. The values of crystallite size calculated were 8.41 nm along the perpendicular direction to (211) crystal planes and 23.7 nm along the perpendicular direction of (002) crystal planes. The planes (211) and (002) were chosen because they are perpendicular to each other. Therefore, the almost 3-fold difference in the crystalline size calculates for each direction plane suggests an anisotropic growth of the particles in the synthesis process. The crystallite size is a measure of the size of coherently diffraction domains and the value of crystallite size cannot be understood as particle size, since a single particle can contain many crystallites.

In order to characterize the morphology of n-HA particles, transmission electron microscopy (TEM) was performed, Figure 1c. TEM image of the n-HA confirms the synthesis of HA nanosized particles. The n-HA particles observed in Figure 1c have structures that resemble needles. This kind of particle shape is also called nanowhiskers. HA with nanowhisker particle shape has many advantages. The high aspect ratio provides improved mechanical properties as fillers in composites. In addition, nanowhiskers particles have higher surface area. The high specific surface area provides a high interaction between phases when HA is used as fillers and it can also be beneficial to higher drug adsorption, when HA is designed to be used as drug carrier.

$\text{N}_2$  sorption isotherms of n-HA are presented in the Figure 1d. BET surface area obtained for n-HA was 67  $\text{m}^2/\text{g}$ . This value of surface area is considered a high value area when compared to values of surface area reported for HA. For instance, HA nanoparticles prepared by sol-gel process can have surface area in the range of 6 to 20  $\text{m}^2/\text{g}$ , as reported by Ziani et al.<sup>45</sup> The  $\text{N}_2$  adsorption/desorption isotherm of n-HA is classified as type V, wherein the adsorbent-adsorbate interaction is weak.<sup>46-48</sup> The isotherm also shows a hysteresis region which is classified as the H1 type, which is often related to rigid porous material with a narrow pore size distribution.<sup>49, 50</sup> The pore diameter of the n-HA calculated by the BJH method was ca. 31 nm, which characterizes n-HA as a mesoporous material. Thereby, n-HA is a promising material for adsorption of drugs.<sup>51</sup>

### 3.2. Terbinafine encapsulation efficiency (EE)

The incorporation of TB on the n-HA was carried out by adsorption of the TB from a solution 2.5 mg/mL of TB in ethanol/water mixtures (5.5/4.5 v/v). For this experiment, the encapsulation efficiency was calculated according to Equation 1. The n-HA are dispersed in a solution in an appropriated amount of n-HA to result in a 5% of TB/n-HA (in weight). The results indicated that the encapsulation efficiency was 77.5%. It means that 77.5% of all TB presented in the ethanol:water solution was adsorbed on the n-HA. Consequently, the TB loading on the n-HA was 40.63 mg per gram of n-HA. In other words, the incorporation of TB onto the n-HA generates a solid material, in which the concentration of TB is 3.9% w/w.

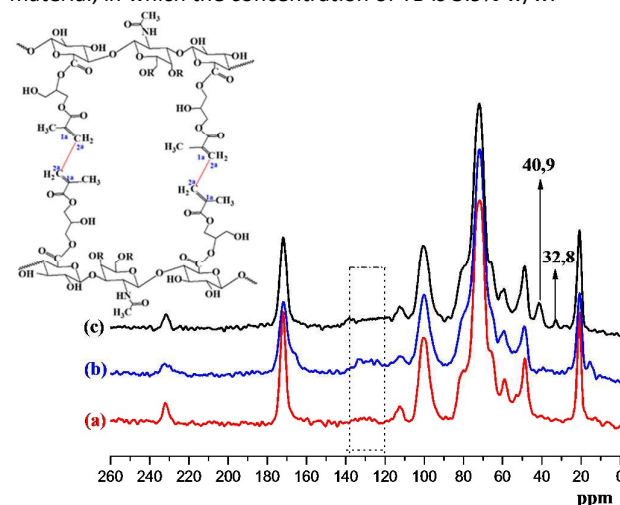


**Figure 2.**  $^{13}\text{C}$ -CP/MAS NMR spectra of CS (a), CS-methacrylate (b) and n-HA-CS microspheres (c).

### 3.3. Synthesis of n-HA/biocompatible polymer microspheres.

The incorporation of n-HA into biocompatible polymer microspheres is tested here as an approach for its application in drug delivery system. CS-methacrylate was used in the synthesis of microspheres, which has methacrylate groups in its structure, so the polysaccharide has double bonds. Therefore, polymerization reaction can be performed promoting the cross-linking of the structure. The chemical

modification of CS is presented and discussed in the supporting information.

Emulsion reticulation reactions are used to the synthesis of polymeric microspheres. Emulsions are thermodynamically stable isotropic systems between two immiscible liquids, stabilized by a surfactant, located in the hydrophobic/hydrophilic interface.<sup>52</sup> The surfactants reduce the interfacial tension between two phases, and they are essential to the stabilization of emulsions. However, in the synthesis of the microspheres, surfactant was not used, since CS has already emulsifying property by itself.

The polymerization occurs because sodium persulfate, in aqueous media, dissociates into free radicals. The free radicals formed attack double bonds of the CS-methacrylate, promoting free radical cross-linking reaction.

The cross-linking process of CS-methacrylate was characterized by <sup>13</sup>C-CP/MAS NMR, Figure 2. In the spectrum of n-HA-CS microspheres, Figure 2 (c), it is possible to observe the appearance of two signals at 40.9 ppm and 32.8 ppm, that were attributed to saturated carbons (CH<sub>2</sub>-C). During the cross-linking reaction, the vinyl groups (C=C) of CS-methacrylate are converted into saturated carbons (C-CH<sub>2</sub>), (Carbon 1a, and Carbon 2a in the structure). It is also possible to observe the absence of the signal at 165 ppm, attributed to carbonyl groups (C=O) from conjugated systems and the absence of signals in the spectral range of 141-120 ppm, which indicates the complete conversion of vinyl groups<sup>53</sup>. The polymerization in emulsion via ultrasound is an extremely efficient method for this type of reaction.

The microspheres containing n-HA was morphologically characterized by SEM. Figure 3 shows the SEM micrographs and the particle size distribution curves of n-HA-CS microspheres containing 1% n-HA (a), 3% n-HA (b), 5% n-HA (c), 7% n-HA (d) and 10% n-HA (e). It is possible to observe microspheres formed for each one of the synthesized samples. The particles size distribution shows that the average particles size varies among 2.8 to 3.7 μm. Comparing the samples morphologies, in terms of size, uniformity and roundness, it was observed that all of the microspheres synthesized from cross-linking CS-methacrylate had diameters near to 3.5 μm, which is an important feature for application as devices for controlled release, since particles of regular shape ensures that drug release is more predictable and stable<sup>54</sup>. The particles size distribution is broad for all condition tested. The formation of spheres with sizes irregular can be associated with a vigorous vibration was applied due to ultrasound. However, a broad size distribution of microsphere can result in an interesting feature for drug release, since it can lead to a broader release pattern.

The presence and the distribution of n-HA in the CS microspheres was studied using TEM. TEM images of the n-HA-CS microspheres containing 10% of n-HA is presented in the Figure 4. n-HA presence in the final materials is straightforward attested by the high contrast difference between the crystalline structure of n-HA and the amorphous polymeric matrix. HA particles, in the form of nanowhiskers, are distributed inside the spherical microparticles. It can be

observed that the degree of aggregation of the nanowhiskers is quite low since many isolated nanowhiskers are observed inside the particles. The presence of isolated n-HA is an indicative of excellent dispersion of the n-HA s inside the microsphere if compared to the initial of the n-HA particles that easily tend to form aggregates. Therefore, the ultrasound waves have effectively contributed to disaggregate the nanowhiskers bundles, and to encapsulate them.

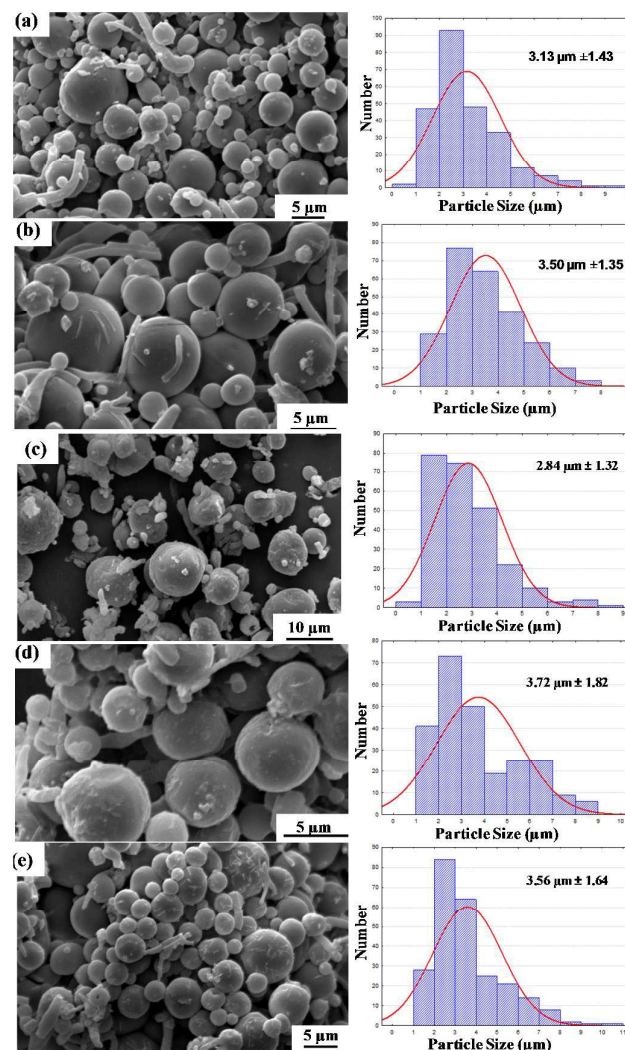


**Figure 3.** Scanning electron microscopy (SEM) images and particle size distribution curves elaborated by measuring sphere sizes for 400 spheres of n-HA-CS microspheres containing 1% n-HA (a), 3% n-HA (b), 5% n-HA (c), 7% n-HA (d) and 10% n-HA (e).

The main issue in the application of HA nanoparticles for drug delivery is its low dispersibility. Then, the colloidal stability of the microspheres containing different loads of n-HA was analyzed. In the Figure 5 is shown the dispersion of n-HA and n-HA-CS microspheres loaded with 1%, 3%, 5%, 7% and 10% of n-HA in distilled water after one minute and after one hour of resting time. Even i for 1 minute of resting time, n-HA is only

slightly dispersed in the solution and almost completed precipitate. Meanwhile, the microspheres are fully dispersed in aqueous medium. After one hour, it can be seen that n-HA is completely precipitated, while the microspheres are kept dispersed in the solution. Thus, it is possible to affirm that the synthesis of microspheres around the n-HA is an excellent strategy to improve the dispersibility of these particles, and the aggregation of n-HA is no longer a concern in the application of n-HA in drug delivery systems.

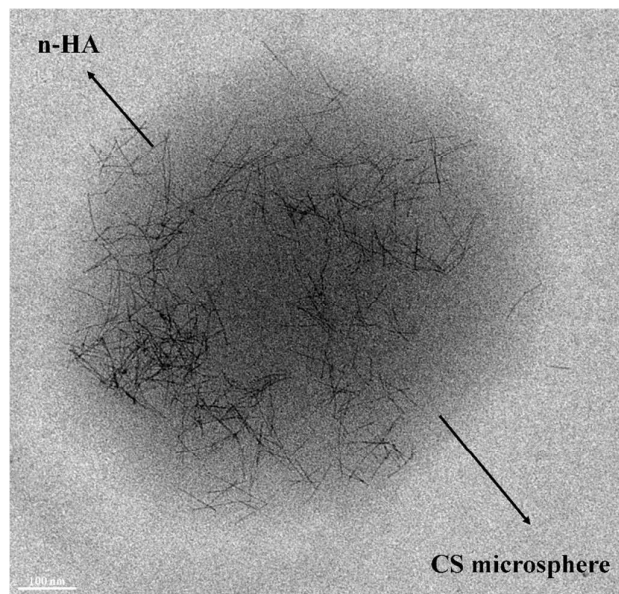


**Figure 4.** Transmission electron microscopy (TEM) images of n-HA-CS microspheres containing 10% of n-HA.

#### 3.4. Release of terbinafine from the microspheres in simulated gastric fluid and simulated intestinal fluid environment

The release profile of TB was evaluated correlating the fraction of drug released in function of time. Time-dependent release curves were calculated through the concentration of drug released at specific time.<sup>55-57</sup> The results are presented in percentage in relation to the total amount of TB encapsulated. In the Figure 6 are shown the time-dependent release curves of TB in SGF and SIF of the microspheres containing 3%, 5%, 7% and 10% n-HA. TB loading in the microspheres depends on the relative amount of HA. TB was incorporated in the microsphere through its adsorption on n-HA. It was found that 40.63 mg of TB was incorporated per gram of n-HA. Consequently, the time-dependent release curves of TB for the microspheres containing 1% n-HA was absent, once a low amount of TB is present in these microspheres.

For the samples containing from 3% to 10% of n-HA, the levels of the drug released in both physiological medium are sustained throughout the experiment. Release patterns observed for the samples are classified as delayed release without initial lag time associated with sigmoidal release at low release time. The sigmoidal component is not clearly observed for sample containing 3% of n-HA, but more intense at higher n-HA content. The release speeds in both SIF and SGF

are similar for the sample contain 3% n-HA, but it is observed a faster release in SGF for the samples with higher n-HA content. At 5 hours of released in SGF, 32.0, 49.6, 55.3, and 54.6% of the TB were released for the materials containing 3, 5, 7 and 10% of n-HA, respectively. The specific time of 5 hours is taken in consideration as an estimative of the time for 50% of colonic filling considering an average gastrointestinal transit time.<sup>58</sup> Therefore, the microspheres containing 3% n-HA showed to be the best tested material considering specific delivery at the colon, with 68% of the TB is still available in the microspheres to be released in the colon.

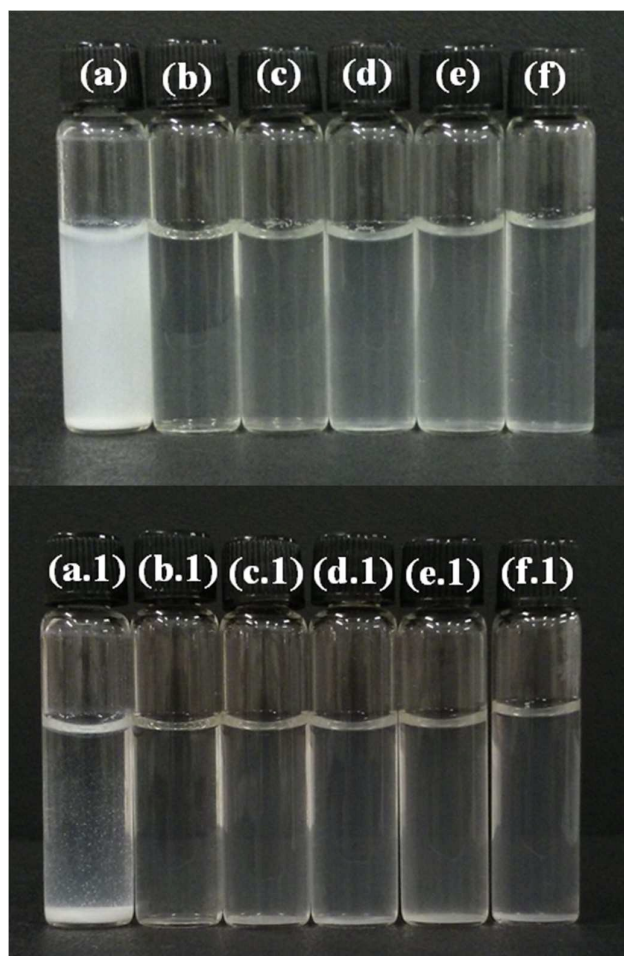


**Figure 5.** Photographs of dispersion of n-HA (a) and n-HA-CS microspheres containing 1% (b), 3% (c), 5% (d), 7% (e) and 10% (f) of n-HA in distilled water after one minute without stirring and (a-1), (b-1), (c-1), (d-1), (e-1) and (f-1) after one hour.

Extending the release time to obtain the equilibrium point, Figure S8, it was found that the mass percentages of TB released from the microspheres in SGF in equilibrium were 87.3% for microspheres containing 3%, 91.0% for microspheres containing 5%, 94.5% for microspheres containing 7% and 93.1% for microspheres containing 10% n-HA. In SIF the mass percentages released of TB were 69.1%,

71.5%, 74.4% and 77.2% for microspheres containing 3%, 5%, 7% and 10% of n-HA, respectively.

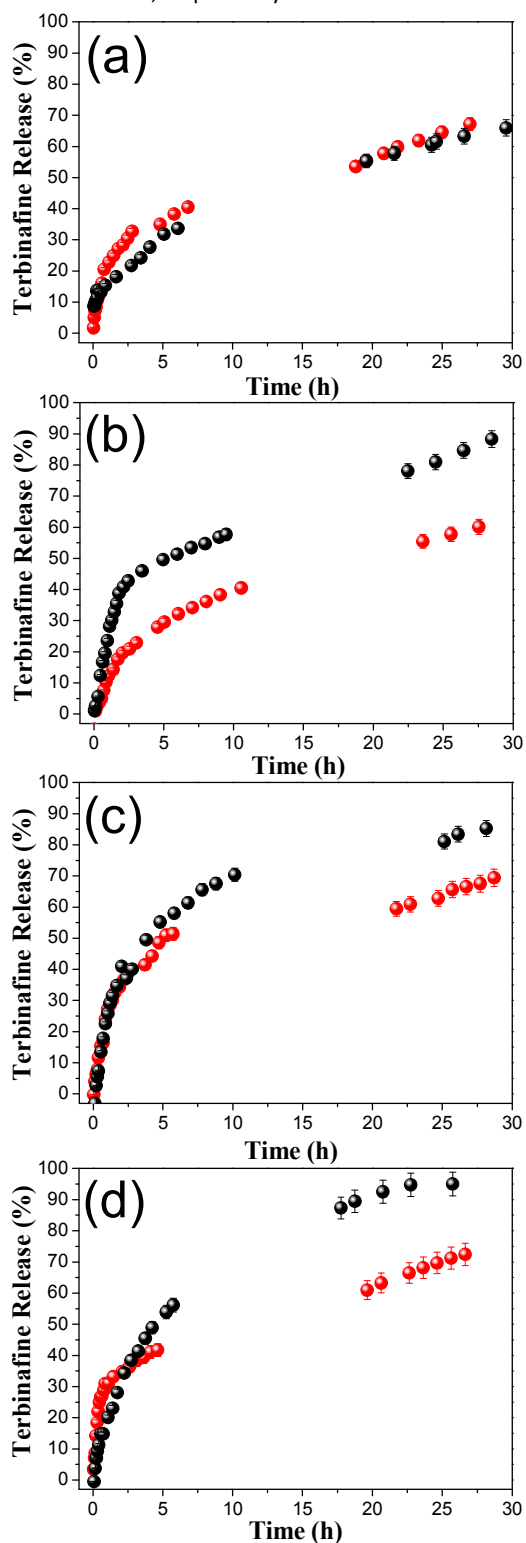


**Figure 6.** Time-dependent release curves of Terbinafine in SGF (black) and SIF (Red) from microspheres containing 3% (a), 5% (b), 7% (c) and 10% (d) of n-HA.

The relative amount of TB released from the microspheres containing n-HA demonstrate that microspheres can deliver a high proportion of their initial load to the specific site of action. Although the stomach offers a narrow therapeutic window for many drugs, the chondroitin sulfate microspheres showed a sustained release rate of TB in the acid medium. Whereas the chondroitin sulfate is only degraded in the colon and can go through different pH values without suffering decomposition, after the time taken to food to transit throughout the stomach, the microspheres can continue releasing the drug in the intestine, since the microspheres also were effective to release TB in intestinal physiological environment.

## Conclusion

HA nanoparticles were successfully synthesized by the method of precipitation in solution, obtaining nanoparticles with crystallite size of 8.41 nm along the perpendicular direction to (211) crystal planes and 23.7 nm along the perpendicular direction of (002) crystal planes. The nanoparticles presented nanowhisker geometry, which has a great interest, since they have improved mechanical properties in the n-HA relation to other geometries. BET surface area obtained for n-HA was ca.  $67 \text{ m}^2/\text{g}$ , which is considered a high value area when compared to others reported in literature. Thereby, n-HA synthesized here is a promising material for adsorption of drugs. n-HA have been shown effective adsorption of terbinafine, in which 77.5% of the drug was adsorbed (ca. 40.63 mg of TB per gram of n-HA).

The chemical modification of CS with GMA was confirmed by FTIR,  $^1\text{H}$  NMR,  $^{13}\text{C}$  NMR, and  $^{13}\text{C}$ -CP/MAS NMR. The synthesis of microspheres by cross-linking CS methacrylate via ultrasound was confirmed by  $^{13}\text{C}$ -CP/MAS NMR proved to be an efficient method in both the cross-linking and the formation of spherical particles with size approximately of  $3.5 \mu\text{m}$ . The approach used in the cross-linking using ultrasound emulsion, it is a novel methodology to date for CS.

The inclusion of n-HA in the spheres showed an interesting alternative to use n-HA in drug release system once the microspheres are fully dispersed in aqueous media while the n-HA is completely precipitated and cannot sustain the drug release.

Furthermore, the microspheres containing n-HA proved to be excellent drug delivery vehicles, releasing about 90% in SGF and about 70% in SIF. Thus, the releasing of terbinafine occurred in both simulated fluid, then after remaining in the stomach, the microspheres may continue releasing the drug in other physiological environment, since a chondroitin sulfate degrades only in the colon by anaerobic bacteria, *Bacteroides thetaiotaomicron ovatus* and *B. fragilis species A*.

## Acknowledgements

T.S.P.C thanks the Conselho Nacional de Desenvolvimento Científico e Tecnológico (CNPq-Brasil) for doctorate

fellowships. A.F.R acknowledges the financial supports given by CNPq, Coordenação de Aperfeiçoamento de Pessoal de Nível Superior (CAPES-Brasil) and Fundação Araucária-Brasil.

## Notes and references

- M. E. Davis, Z. Chen and D. M. Shin, *Nature Reviews Drug Discovery*, 2008, **7**, 771-782.
- P. Gou, W. Liu, W. Mao, J. Tang, Y. Shen and M. Sui, *Journal of Materials Chemistry B*, 2013, **1**, 284-292.
- R. Gaspar and R. Duncan, *Adv. Drug Deliv. Rev.*, 2009, **61**, 1220-1231.
- K. Itaka, T. Ishii, Y. Hasegawa and K. Kataoka, *Biomaterials*, 2010, **31**, 3707-3714.
- Y. Du, W. Ren, Y. Li, Q. Zhang, L. Zeng, C. Chi, A. Wu and J. Tian, *Journal of Materials Chemistry B*, 2015, **3**, 1518-1528.
- M. Chen, X. He, K. Wang, D. He, S. Yang, P. Qiu and S. Chen, *Journal of Materials Chemistry B*, 2014, **2**, 428-436.
- Z. Zhao, H. Zhang, X. Chi, H. Li, Z. Yin, D. Huang, X. Wang and J. Gao, *Journal of Materials Chemistry B*, 2014, **2**, 6313-6323.
- Z. P. Xu, Q. H. Zeng, G. Q. Lu and A. B. Yu, *Chem. Eng. Sci.*, 2006, **61**, 1027-1040.
- I. Nadra, J. C. Mason, P. Philippidis, O. Florey, C. D. W. Smythe, G. M. McCarthy, R. C. Landis and D. O. Haskard, *Circ.Res.*, 2005, **96**, 1248-1256.
- Y. R. Cai and R. K. Tang, *J. Mater. Chem.*, 2008, **18**, 3775-3787.
- R. Rodriguez-Clemente, A. Lopez-Macipe, J. Gomez-Morales, J. Torrent-Burgues and V. M. Castano, *Journal of the European Ceramic Society*, 1998, **18**, 1351-1356.
- P. Koutsoukos, Z. Amjad, M. B. Tomson and G. H. Nancollas, *J. Am. Chem. Soc.*, 1980, **102**, 1553-1557.
- M. J. Olszta, X. Cheng, S. S. Jee, R. Kumar, Y.-Y. Kim, M. J. Kaufman, E. P. Douglas and L. B. Gower, *Materials Science & Engineering R-Reports*, 2007, **58**, 77-116.
- A. Belcarz, A. Zima and G. Ginalska, *International Journal of Pharmaceutics*, 2013, **454**, 285-295.
- H. Miyazaki, H. Maeda, S. Yoshida, H. Suzuki and T. Ota, *J. Ceram. Soc. Jpn.*, 2014, **122**, 835-837.
- W. Suchanek and M. Yoshimura, *J. Mater. Res.*, 1998, **13**, 94-117.
- K. Yamamura and T. Yotsuyanagi, *International Journal of Pharmaceutics*, 1992, **79**, R1-R3.
- D. Schmaljohann, *Adv. Drug Deliv. Rev.*, 2006, **58**, 1655-1670.
- H. Liu, X.-G. Yang, S.-F. Nie, L.-L. Wei, L.-L. Zhou, H. Liu, R. Tang and W.-S. Pan, *International Journal of Pharmaceutics*, 2007, **332**, 115-124.
- V. R. Sinha and R. Kumria, *European Journal of Pharmaceutical Sciences*, 2003, **18**, 3-18.
- J. S. Pieper, P. B. van Wachem, M. J. A. van Luyn, L. A. Brouwer, T. Hafmans, J. H. Veerkamp and T. H. van Kuppevelt, *Biomaterials*, 2000, **21**, 1689-1699.
- K. V. Phadke, L. S. Manjeshwar and T. M. Aminabhavi, *Polymer Bulletin*, 2014, **71**, 1625-1643.
- E. P. da Silva, D. L. A. Sitta, V. H. Fragal, T. S. P. Cellet, M. R. Mauricio, F. P. Garcia, C. V. Nakamura, M. R. Guilherme, A. F. Rubira and M. H. Kunita, *International Journal of Biological Macromolecules*, 2014, **67**, 43-52.
- J. Lee and H.-S. Yun, *Journal of Materials Chemistry B*, 2014, **2**, 1255-1263.
- M. T. Al Samri, R. Silva, S. Almarzooqi, A. Albawardi, A. R. D. Othman, R. S. M. S. Al Hanjeri, S. K. M. Al Dawaar, S. Tariq, A.-K. Souid and T. Asefa, *International Journal of Nanomedicine*, 2013, **8**, 1223-1244.
- R. Li, F. Feng, Y. Wang, X. Yang, X. Yang and V. C. Yang, *J. Colloid Interface Sci.*, 2014, **429**, 34-44.
- W. J. Liu and Z. C. Zhang, *Polym. Compos.*, 2010, **31**, 1846-1852.
- C. Kojima, K. Watanabe, T. Nagayasu, Y. Nishio, R. Makiura and A. Nakahira, *Journal of Nanoparticle Research*, 2013, **15**.
- S. Jose, S. S. Anju, T. A. Cinu, N. A. Aleykutty, S. Thomas and E. B. Souto, *International Journal of Pharmaceutics*, 2014, **474**, 6-13.
- R. K. Subedi, K. W. Kang and H.-K. Choi, *European Journal of Pharmaceutical Sciences*, 2009, **37**, 508-513.
- Z. H. Xu, L. L. Chen, W. W. Gu, Y. Gao, L. P. Lin, Z. W. Zhang, Y. Xi and Y. P. Li, *Biomaterials*, 2009, **30**, 226-232.
- L. F. Wang, S. S. Shen and S. C. Lu, *Carbohydrate Polymers*, 2003, **52**, 389-396.
- J. Q. Xi, L. Zhou and Y. H. Fei, *Int. J. Biol. Macromol.*, 2012, **50**, 157-163.
- D. M. Fernandes, A. A. W. Hechenleitner, M. F. Silva, M. K. Lima, P. R. S. Bittencourt, R. Silva, M. A. C. Melo and E. A. G. Pineda, *Materials Chemistry and Physics*, 2009, **118**, 447-452.
- D. M. Fernandes, R. Silva, A. A. W. Hechenleitner, E. Radovanovic, M. A. C. Melo and E. A. G. Pineda, *Materials Chemistry and Physics*, 2009, **115**, 110-115.
- W. J. Nascimento, T. G. M. Bonadio, V. F. Freitas, W. R. Weinand, M. L. Baesso and W. M. Lima, *Materials Chemistry and Physics*, 2011, **130**, 84-89.
- R. Silva and T. Asefa, *Advanced Materials*, 2012, **24**, 1878-1883.
- R. Silva, A. V. Biradar, L. Fabris and T. Asefa, *J. Phys. Chem. C*, 2011, **115**, 22810-22817.
- W. R. Walsh and N. Guzelsu, *Biomaterials*, 1994, **15**, 137-145.
- I. Rehman and W. Bonfield, *Journal of Materials Science-Materials in Medicine*, 1997, **8**, 1-4.
- R. Silva, G. M. Pereira, E. C. Muniz and A. F. Rubira, *Crystal Growth & Design*, 2009, **9**, 3307-3312.
- J. Huang, Y. W. Lin, X. W. Fu, S. M. Best, R. A. Brooks, N. Rushton and W. Bonfield, *Journal of Materials Science-Materials in Medicine*, 2007, **18**, 2151-2157.
- C. Kothapalli, M. Wei, A. Vasiliev and M. T. Shaw, *Acta Materialia*, 2004, **52**, 5655-5663.
- S. Zadeqan, M. Hosainalipour, H. R. Rezaie, H. Ghassai and M. A. Shokrgozar, *Materials Science & Engineering C-Materials for Biological Applications*, 2011, **31**, 954-961.
- S. Ziani, S. Meski and H. Khireddine, *International Journal of Applied Ceramic Technology*, 2014, **11**, 83-91.
- A. Singh, *Bulletin of Materials Science*, 2012, **35**, 1031-1038.
- Z. Xu, C. Liu, J. Wei and J. Sun, *Journal of Applied Toxicology*, 2012, **32**, 429-435.
- S. Kongsri, K. Janpradit, K. Buapa, S. Techawongstien and S. Chanthai, *Chemical Engineering Journal*, 2013, **215**, 522-532.

## ARTICLE

Journal Name

49. D. Y. Zhao, Q. S. Huo, J. L. Feng, B. F. Chmelka and G. D. Stucky, *Journal of the American Chemical Society*, 1998, **120**, 6024-6036.
50. D. Y. Zhao, J. L. Feng, Q. S. Huo, N. Melosh, G. H. Fredrickson, B. F. Chmelka and G. D. Stucky, *Science*, 1998, **279**, 548-552.
51. U. Ciesla and F. Schuth, *Microporous and Mesoporous Materials*, 1999, **27**, 131-149.
52. A. G. DeOliveira, M. V. Scarpa and H. Chaimovich, *Journal of Pharmaceutical Sciences*, 1997, **86**, 616-620.
53. M. R. Guilherme, A. V. Reis, B. R. V. Alves, M. H. Kunita, A. F. Rubira and E. B. Tambourgi, *Journal of Colloid and Interface Science*, 2010, **352**, 107-113.
54. M. Li, O. Rouaud and D. Poncelet, *International Journal of Pharmaceutics*, 2008, **363**, 26-39.
55. P. L. Ritger and N. A. Peppas, *Journal of Controlled Release*, 1987, **5**, 23-36.
56. P. L. Ritger and N. A. Peppas, *Journal of Controlled Release*, 1987, **5**, 37-42.
57. R. W. Korsmeyer, R. Gurny, E. Doelker, P. Buri and N. A. Peppas, *International Journal of Pharmaceutics*, 1983, **15**, 25-35.
58. M. Camilleri, L. J. Colemont, S. F. Phillips, M. L. Brown, G. M. Thomforde, N. Chapman and A. R. Zinsmeister, *American Journal of Physiology*, 1989, **257**, G284-G290.

